Synthesis and Characterization of $AlPO_4$-36 and MAPO-36 with Different Magnesium Content

Marina da S. Machado and Dilson Cardoso*

Federal University of São Carlos, Chemical Engineering Department, P.O. Box 676, São Carlos 13.565-905, SP., Brazil

Joaquín Pérez-Pariente and Enrique Sastre

Instituto de Catálisis y Petroleoquímica, CSIC, Camino de Valdelatas, Campus Universidad Autónoma, 28049 Cantoblanco, Madrid, Spain

Received May 19, 1999. Revised Manuscript Received September 15, 1999

The objective of this work was to perform a systematic study regarding the effect of different synthesis parameters on the crystallization of $AlPO_4$-36 and MAPO-36 (aluminophosphate molecular sieve type 36, ATS, structure). MAPO-36 samples were synthesized from gels containing different magnesium contents in order to obtain catalysts with different degrees of acidity. Under the synthesis conditions employed in this work, the formation of $AlPO_4$-36 and MAPO-36 increased when the reaction mixture was aged at room temperature; however, small amounts of $AlPO_4$-5 always crystallize parallel to the ATS materials. The presence of magnesium in the reaction mixture can also favor the formation of the ATS structure; nevertheless, the synthesis of pure MAPO-36 from reaction mixtures having very low magnesium content was not possible under several conditions. Pseudoboehmite was a better aluminum source than aluminum isopropoxide for the formation of MAPO-36. A practically pure ATS structure was obtained from reaction mixtures containing molar fractions of Mg between 0.033 and 0.133. For higher magnesium contents, traces of another unidentified phase were detected. Energy-dispersive spectrometry analysis indicates a uniform chemical composition of the MAPO-36 particles, and Scanning electron microscopy shows that the ATS samples have a needlelike morphology. Thermogravimetric analysis of ATS samples reveals that the weight loss corresponding to the decomposition of protonated amine is linearly correlated with magnesium content in the solid up to 0.8 mmol of magnesium per gram of solid.

Introduction

The structure of aluminophosphate molecular sieve type 36 (ATS) is characterized by a one-dimensional system of channels parallel to the *c*-axis and micropores formed by 12-ring tetrahedral apertures.[1] The pores have an elliptical shape with dimensions of 7.4 × 6.5 Å[1] and, because of the presence of side pockets inside the channels, these dimensions are enlarged to 10.1 × 9.2 Å.[1] In MAPO-36, part of the aluminum atoms of $AlPO_4$-36 are substituted by magnesium, generating a negatively charged framework and resulting in ion exchange capacity and the possibility of forming Brönsted acidity.[2,3]

Materials having ATS structure can be synthesized from gels containing tripropylamine as organic template, although this template can also direct the formation of $AlPO_4$-5.[2,4,5] Therefore, as recently stated by Kaliaguine et al.,[6] it is very difficult to obtain $AlPO_4$-36 as a pure phase, because $AlPO_4$-5 (AFI) is also frequently formed competitively. The study of MAPO-36 is very interesting as this magnesium-containing material presents higher acidity than when it is obtained with other metals substituted in ATS structure.[7,8] MAPO-36 is also interesting as it presents higher acid strength compared to other large-pore aluminophosphate molecular sieves such as SAPO-5 and MAPO-5 containing the same concentration of substituted element.[8,9]

For these reasons, the objective of this work was to perform a systematic study regarding the effect of different synthesis parameters on the crystallization of $AlPO_4$-36 and MAPO-36 and their characterization by means of several physicochemical techniques. MAPO-36 samples were synthesized from gels containing different magnesium contents in order to obtain catalysts with distinct degrees of acidity.

Experimental Section

Synthesis of $AlPO_4$-36. $AlPO_4$-36 was synthesized according to a procedure recently reported by Kaliaguine[6] including

* Corresponding author. E-mail: dilson@power.ufscar.br.

(1) Smith, V. J.; Pluth, J. J.; Andries, J. K. *Zeolites* **1993**, *13*, 166.
(2) Flanigen, E. M.; Lok, B. M.; Patton, L.; Wilson, S. T. *Pure Appl. Chem*. **1986**, *58*, 1531.
(3) Akolekar, D. B. *Zeolites* **1994**, *14*, 53.
(4) Ono, Y.; Nagashiro, K. *J. Chem. Soc., Faraday Trans.* **1991**, *87*, 3309.
(5) Akolekar, D. B. *J. Catal.* **1993**, *143*, 227.
(6) Zahedi Niaki, M. H.; Praphulla, J. N.; Kaliaguine, S. *Chem. Commum*. **1996**, 1373.
(7) Akolekar, D. B. *J. Chem. Soc., Faraday Trans.* **1994**, *90*, 1041.
(8) Akolekar, D. B. *Appl. Catal., A* **1994**, *112*, 125.
(9) Akolekar, D. B. *J. Catal.* **1993**, *144*, 148.

10.1021/cm9903071 CCC: $18.00
Published on Web 10/28/1999

Table 1. Influence of Gel Aging at Ambient Temperature

gel[a]	1st stage[b] (h)	2nd stage[c] (h)	pH[d] initial	pH[d] final	crystallinity ATS	crystallinity AFI
A	0.5	1.0	5.1	7.8	0	100
B	2.0	2.0	5.6	8.0	35	19
C	12.0	6.0	6.6	8.5	40	15

[a] Gel composition: 1.7 Pr_3N:Al_2O_3:P_2O_5:80 H_2O. [b] Reaction mixture: water, phosphoric acid, and aluminum source. [c] Addition of amine to the reaction mixture. [d] Before and after crystallization.

however some slight modifications: the aging time of the gel at room temperature and the template content.

In the study on gel aging, a composition of 1.7 Pr_3N:Al_2O_3:P_2O_5:80 H_2O was employed. The gels were prepared according to the following procedure. First stage: phosphoric acid (H_3PO_4, Riedel de Haën 85 wt %) was diluted in deionized water and pseudoboehmite (74.6% Al_2O_3, Pural SB, Condea) was added, obtaining in this manner a suspension that was aged under stirring. Second stage: after aging, tripropylamine (Aldrich 98 wt %) was added dropwise to this suspension. Three different aging times were employed giving gels A−C (Table 1). The gels were then transferred to Teflon-lined stainless steel autoclaves and submitted to crystallization under static conditions in two temperature steps, namely at 393 K for 5 days and subsequently at 413 K for 3 days.

In the study of the influence of template content gels with composition x Pr_3N:Al_2O_3:P_2O_5:80 H_2O were employed with x varying from 1.6 to 2.2. After aging according to procedure C (Table 1), the gels were left to crystallize under the conditions stated above.

To obtain a pure $AlPO_4$-36 phase, the best sample containing traces of $AlPO_4$-5 (gel C, Table 1) was submitted to stirring, decanting, and centrifuging. As the $AlPO_4$-36 crystals are smaller than those of $AlPO_4$-5, the two phases could be separated from each other, obtaining an $AlPO_4$-36 yield of about 30% of initially used solid.

Synthesis of MAPO-36. The materials used to synthesize MAPO-36 were the same as those utilized for the $AlPO_4$-36 but with the addition of the necessary amount of magnesium acetate tetrahydrate (99 wt % Aldrich). To verify the effect of the aluminum source, in some synthesis, aluminum isopropoxide (98 wt % Aldrich) was used instead of pseudoboehmite. The MAPOs were obtained from reaction mixtures with the following chemical composition:

$$x\ Pr_3N{:}2y\ MgO{:}(1-y)Al_2O_3{:}P_2O_5{:}40\ H_2O{:}4y\ HOAC{:}6(1-y)\text{i-PrOH} \quad (1)$$

In eq 1, i-PrOH stands for isopropyl alcohol formed when aluminum isopropoxide is used as aluminum source and is generally not removed from the reaction medium.[5] The sum of magnesium and aluminum content in the gels were maintained constant and were always equal to the sum of phosphorus, assuming that an MS1 mechanism takes place in the MAPO formation, where magnesium substitutes only the aluminum.[2] The general synthesis procedure utilized was based on that employed by Ono and Nagashiro[4] and Akolekar,[5] however modifying the aging time of the gel at room temperature. When aluminum isopropoxide was used as the aluminum source, the aging method B was employed (Table 1). Because pseudoboehmite is less reactive, a larger aging time was used for the syntheses employing this material (gel C, Table 1). The gels were transferred to Teflon-lined stainless steel autoclaves and crystallized under static conditions, generally using the following steps: initially, for 50 h at 373 K and then 24 h at 423 K. In the case of gels obtained using pseudoboehmite and low magnesium content, the effect of the crystallization conditions were also studied because Kaliaguine et al.[6] observed that aging at 393 K for 5 days seems to be a determinant factor in the formation of ATS materials.

In all cases, the solid product obtained was centrifuged, washed, and dried in an oven at 333 K and stored under ambient conditions.

Table 2. Synthesis Results Using Aluminum Isopropoxide[a]

sample	Mg/(Mg+Al+P) gel	Mg/(Mg+Al+P) solid	amine (x)	pH[b] initial	pH[b] final	solid yield[c]	crystallinity % ATS	crystallinity % AFI
I01	0.033	nd	1.0	6.8	8.4	15.0	31	70
I02	0.033	nd	1.4	7.3	8.6	14.3	38	51
I03	0.033	0.026	1.8	7.9	8.7	13.0	70	10
I04	0.033	0.035	2.0	8.0	8.7	14.3	80	0
I06	0.053	nd	1.0	6.6	8.2	15.6	25	73
I07	0.053	nd	1.4	7.2	8.3	13.6	33	69
I08	0.053	0.052	1.8	7.7	8.5	14.0	90	0
I09	0.053	0.061	2.0	7.8	8.4	14.7	100	0
I10	0.058	nd	1.8	7.3	8.5	15.4	61	21
I12	0.058	nd	2.4	8.0	8.4	14.3	87	13
I13	0.058	nd	2.8	8.3	8.6	15.3	85	11
I16	0.063	nd	1.8	7.3	8.4	15.3	56	37
I19	0.063	nd	2.4	8.1	8.2	14.1	65	28
I20	0.063	nd	2.8	8.2	8.1	13.6	66	26
I21	0.075	nd	1.8	7.2	8.2	14.5	40	58
I24	0.075	nd	2.4	7.8	8.0	14.4	53	41
I25	0.075	nd	2.8	8.0	7.7	14.8	51	40

[a] Crystallization conditions: 50 h at 373 K and 24 h at 423 K. [b] Before and after crystallization. [c] Solid (g) per 100 g of reaction mixture.

Characterization. The X-ray diffractograms (XRD) of the samples were obtained in a Philips PW 1710 diffractometer using Cu−Kα radiation. The crystallinity of the materials was estimated by eq 2:

$$y = \frac{100\sum_{i=1}^{n} I(\text{sample})}{\sum_{i=1}^{n} I(\text{patron})} \quad (2)$$

The ATS crystallinity was determined from the ratio between the sum of the peaks intensities that appear at $2\theta =$ 15.79, 16.43, 19.06, 20.69, 27.14, 27.22, 27.78, and 28.29 (eq 2, $n = 8$) and those of the standard sample (I09, Table 2). The percentage of AFI in the solids was determined by dividing the area of the peaks ($n = 3$) that appear at $2\theta = 14.89$, 19.74, and 25.94 by the area of the same peaks of a 100% crystalline MAPO-5 containing 1.4 mol % of Mg in the solid.

Elemental analysis of aluminum, magnesium and phosphorus was determined by plasma emission induced spectrophotometry. Scanning electron microscopy (SEM) and energy-dispersive spectrometry (EDX) microanalysis were performed in a Zeiss DSM 960 microscope and an EDX Link Analytical QX2000 microanalyzer, respectively. EDX analysis was performed from the powder and from five distinct particles of each sample. For the standard sample (I09), a 40 μm long particle was mapped, analyzing 10 points along its length. Thermal analysis (TG/DTG/DTA) was carried out in oxidizing atmosphere, using a Perkin-Elmer TGA 7 and DTA 7, at a temperature range of 303−1173 K, with an approximately 10 mg sample. A heating rate of 10 K/min was used with an air flow rate of 30 cm^3/min.

Results and Discussion

Synthesis Results. For the $AlPO_4$-36 samples synthesized using pseudoboehmite as an Al source (Table 1), gel aging under stirring at room temperature substantially affected the final product. With an increase in the aging time before and after the addition of amine (first and second stages, respectively), more $AlPO_4$-36 is obtained; however it was contaminated with at least 15% $AlPO_4$-5. Neither an increase nor a decrease in the organic template content ($x = 1.5$, 2.0, 2.2) in gel C nor

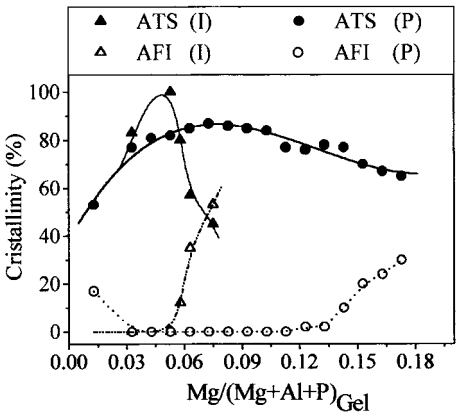

Figure 1. Crystallinity as a function of Mg in the gel. I = Al−isopropoxide ($x = 2.0$) and P = pseudoboehmite ($x = 1.8$).

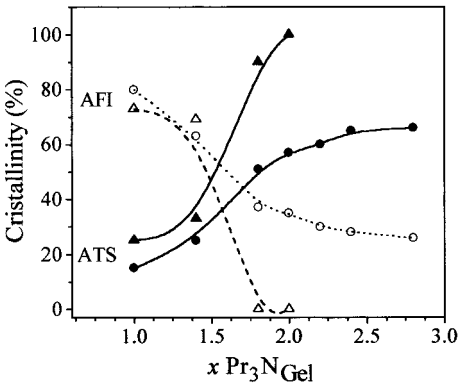

Figure 2. Crystallinity of MAPOs from aluminum isopropoxide as a function of Pr_3N in the gel (for ▲ and △, $y = 0.105$; for ● and ○, $y = 0.125$).

an increase in crystallization time at 413 K for as much as 5 days allowed us to obtain $AlPO_4$-36 less contaminated with $AlPO_4$-5. It may thus be concluded that the gel composition C, under the conditions presented in Table 1, is the best way to obtain $AlPO_4$-36, despite the presence of traces of $AlPO_4$-5. Purification of this sample through decanting and centrifuging of the supernatant phase resulted in a solid showing only $AlPO_4$-36 DRX peaks with a crystallinity of 65% in relation to a standard sample (I09, Table 2).

MAPO samples synthesized using aluminum isopropoxide (Table 2) show that the increase in amine content improves the MAPO-36 crystallinity. For an amine content of $x = 2.0$, pure samples of MAPO-36 (Figure 1) were obtained for a very limited range of Mg/(Mg+Al+P) ratio in the reaction mixture: between 0.033 and 0.053. Figure 1 also shows that the formation of MAPO-5 is favored with increasing magnesium content in the gel.

The effect of template content on MAPO-36 crystallinity for two magnesium values in the reaction mixture and using aluminum isopropoxide is shown in Figure 2. It may be noted that at low template contents the AFI structure is the main solid product and that the formation of the ATS structure is favored as the template contents increase. For each template content, increasing magnesium content favors the formation of MAPO-5, and it is necessary to use higher template contents in order to obtain MAPO-36 with relatively high crystallinity. For the synthesis using high magnesium concentration in the gel, apparently there is a

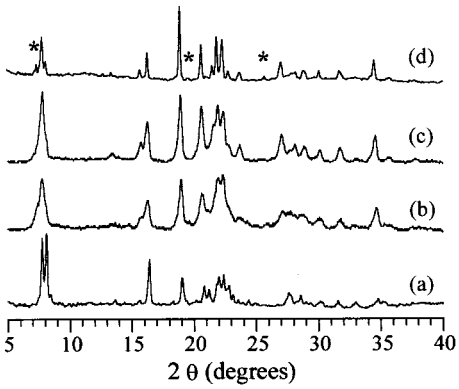

Figure 3. XRD of ATS samples with increasing Mg content: (a) P00, (b) P03, (c) P07, and (d) P14. The asterisks indicate the formation of AFI phase.

Table 3. Synthesis Results Using Pseudoboehmite as Aluminum Source[a]

	Mg/(Mg+Al+P)		pH		solid[b]	crystallinity %	
sample	gel	solid	initial	final	yield	ATS	AFI
P00	0.000	0.000	6.6	8.5	nd	65[c]	0
P01	0.006	nd	7.3	8.1	22.7	0	100
P02	0.013	nd	7.1	8.6	24.5	53	17
P03	0.033	0.025	7.0	8.0	18.6	77	*t*
P04	0.043	0.030	6.9	7.9	22.5	81	*t*
P05	0.053	0.040	6.7	7.9	23.0	82	
P06	0.063	0.042	6.7	7.7	22.1	85	
P07	0.073	0.051	6.5	7.5	22.3	87	
P08	0.083	0.053	6.5	7.5	21.0	86	
P09	0.093	0.057	6.3	7.4	21.6	85	
P10	0.103	nd	6.2	7.6	18.6	84	*t*
P11	0.113	0.074	6.1	7.4	20.1	77	*t*
P12	0.123	nd	6.2	7.4	20.3	76	*t*
P13	0.133	nd	5.8	7.3	17.3	78	*t*
P14	0.143	0.083	5.8	7.3	18.6	77	10
P15	0.153	nd	5.6	7.2	18.3	70	20 + *I*
P16	0.163	nd	5.6	7.2	19.0	67	24 + *I*
P17	0.173	nd	5.5	6.8	20.6	65	30 + *I*

[a] Crystallization conditions (except for P00): $x = 1.8$, 50 h at 373 K and 24 h at 423 K. Key: *t* = traces of MAPO-5, *I* = traces of unidentified phase, and nd = not determined. [b] Solid (g) per 100 g of gel. [c] Sample obtained from gel C, after purification by decanting.

limiting template content above which the crystallinity of MAPO-36 will not be favored anymore. As indicated in Table 2, the initial pH of the reaction mixture increases parallel to the template content, and apparently when the pH value is higher than 7.5, it favors the crystallization of MAPO-36. Concerning the final pH of the crystallization, the results in Table 2 also indicate that for a constant template content (for instance, $x = 1.8$) pH decreases as magnesium increases in the reaction mixture. This pH decrease can be a consequence of a higher acetic acid formation, as indicated in eq 1.

When pseudoboehmite was used as source of aluminum and maintaining a constant template content ($x = 1.8$) practically pure MAPO-36 was obtained for Mg/(Mg+Al+P) ratios between 0.033 and 0.133 (Figures 1 and 3 and Table 3), which is a much wider range than what was permitted when aluminum isopropoxide was used instead (Figure 1 and Table 2). Outside this range, for both lower and higher magnesium contents in the gel, MAPO-5 crystallized together with MAPO-36. For Mg/(Mg+Al+P) ratios above 0.143, besides MAPO-5, traces of an unidentified phase were detected (phase I,

Table 4. Crystallization Time for Gels with Low Mg Content

sample	gel Mg/(Mg+Al+P)	(x)	pH initial	pH final	synthesis conditions	crystallinity % ATS[a]	crystallinity % AFI
P18	0.006	2.4	7.4	8.3	373 K/50 h + 423 K/24 h	0	100
P19	0.006	2.4	7.4	8.4	373 K/120 h + 423 K/48 h	*t*	90
P20	0.006	4.8	7.7		373 K/120 h + 423 K/48 h	*t*	87
P21	0.006	4.8	7.7		373 K/120 h + 423 K/96 h	*t*	86
P22	0.006	4.8	7.7		373 K/168 h + 423 K/96 h	5	86
*P*23	0.013	2.0	7.2	8.7	373 K/50 h + 423 K/24 h	57	15
P24	0.013	2.4	7.3	8.8	373 K/50 h + 423 K/24 h	60	13
P25	0.013	2.4	7.3	8.7	373 K/120 h + 423 K/24 h	61	*t*
P26	0.013	2.4	7.3	8.2	373 K/120 h + 423 K/48 h	65	*t*
P27	0.013	2.4	7.3		373 K/168 h + 423 K/48 h	58	11
P28	0.013	2.4	7.3		373 K/168 h + 423 K/96 h	60	7

[a] *t* = traces of MAPO-36.

Table 3), possibly a nonmicroporous magnesium-rich phosphate as also observed by Akolekar[5] and Giotto et al.[10] Regarding the initial pH of the reaction mixture, when pseudoboehmite is used as aluminum source, it is possible to obtain practically pure MAPO-36 for gels with initial pH values between 5.8 and 7.0, whereas for the synthesis carried out using aluminum isopropoxide, this value is higher and between 7.3 and 8.0 (Tables 2 and 3, respectively).

Because the synthesis of MAPO-36 employing low Mg content results in a high contamination of MAPO-5 (Table 3), in this case, the synthesis conditions were varied more extensively. Tables 3 and 4 shows that for Mg/(Mg+Al+P) = 0.013 an increase in the template content from 1.8 to 2.4 increases slightly the purity of MAPO-36 from 53 to 60% (samples P02 and P24, respectively). Increasing the duration of both crystallization steps, the crystallinity of MAPO-36 increases further to 65%, but in this case, the product has a virtually pure ATS structure (sample P26). Additional increase in the duration of any of these stages does not increase the crystallinity of MAPO-36 and produces contamination with MAPO-5 (samples P27 and P28). Similar results were also reported by Kaliaguine et al.[6] for the synthesis of $AlPO_4$-36, indicating that gel aging has a definite effect on the nature of the final product for the syntheses with low magnesium contents. However, by applying the same systematic synthesis conditions for gels containing less magnesium (Mg/(Mg+Al+P) = 0.006), it was not possible to increase the formation of MAPO-36 to values higher than 5% (samples P18−22).

Chemical Composition. A comparison between the Mg/(Mg+Al+P) values in gel and that of the solid products containing at least 80% MAPO-36 is shown in Figure 4, where the dashed line indicates 100% Mg incorporation. It can be observed that the magnesium content in the solid was in general lower than that in the gel and that the incorporation efficiency of magnesium in the solid decreases with increasing magnesium content in the gel. Furthermore, the (Al+Mg)/P ratios in the solid were always close to unity (Table 5), suggesting that Mg^{2+} substitutes Al^{3+} in the MAPO-36 framework and probably is not present in great extent in cationic positions compensating framework charge.

EDX. The chemical compositions determined by EDX of samples synthesized with aluminum isopropoxide (Table 5) are in good agreement with those obtained by elemental analysis, indicating uniform chemical composition of the MAPO-36 particles. Mapping of a 40 μm particle of sample I09 showed that in all points the ratio Mg/(Mg+Al+P) is practically constant, indicating a homogeneous distribution of magnesium throughout the particle.

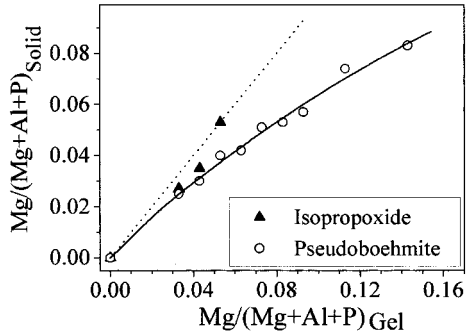

Figure 4. Magnesium content in the solid and in the gel.

Table 5. Chemical Composition for Samples Synthesized with Aluminum Isopropoxide

sample	gel Mg/P	gel Al/P	solid Mg/P		solid Al/P		solid (Mg+Al)/P	
I04	0.065	0.935	0.052[a]	0.055[b]	0.913[a]	0.910[b]	0.97[a]	0.96[b]
I05	0.085	0.915	0.059	0.066	0.930	0.900	0.99	0.97
I08	0.105	0.895	0.102	0.103	0.854	0.880	0.96	0.98

[a] Compositions from elemental analysis. [b] Compositions from EDX.

SEM. Analyses of the morphology of the samples synthesized using pseudoboehmite as aluminum source revealed that the $AlPO_4$-36 is formed by needles (sample P00, Figure 5a). In the case of MAPO-36 samples, these needles agglomerate, giving rise to spherical aggregates (samples P03, P05, and P14, corresponding to micrographs 5b, 5c and 5d, respectively). The diameter of the spherical agglomerates increases as the magnesium content increases, ranging from 20 to 100 μm. The MAPO-36 samples synthesized using aluminum isopropoxide also formed similar aggregates, but their shapes were more irregular.

Thermal Analysis. The TG/DTG/DTA results of some selected samples synthesized from pseudoboehmite are plotted in Figure 6. Figure 6a (sample P00) shows that $AlPO_4$-36 presents four distinct weight-loss stages at the following temperature ranges: I = 300−373 K, II = 373−473 K, III = 473−623 K, IV = 623−

(10) Giotto, M. V.; Machado, M. da S.; Pérez-Pariente, J.; Rios, S. P. O.; Cardoso, D. *11th International Zeolite Conference*; Baltimore, 1998; p 2481.

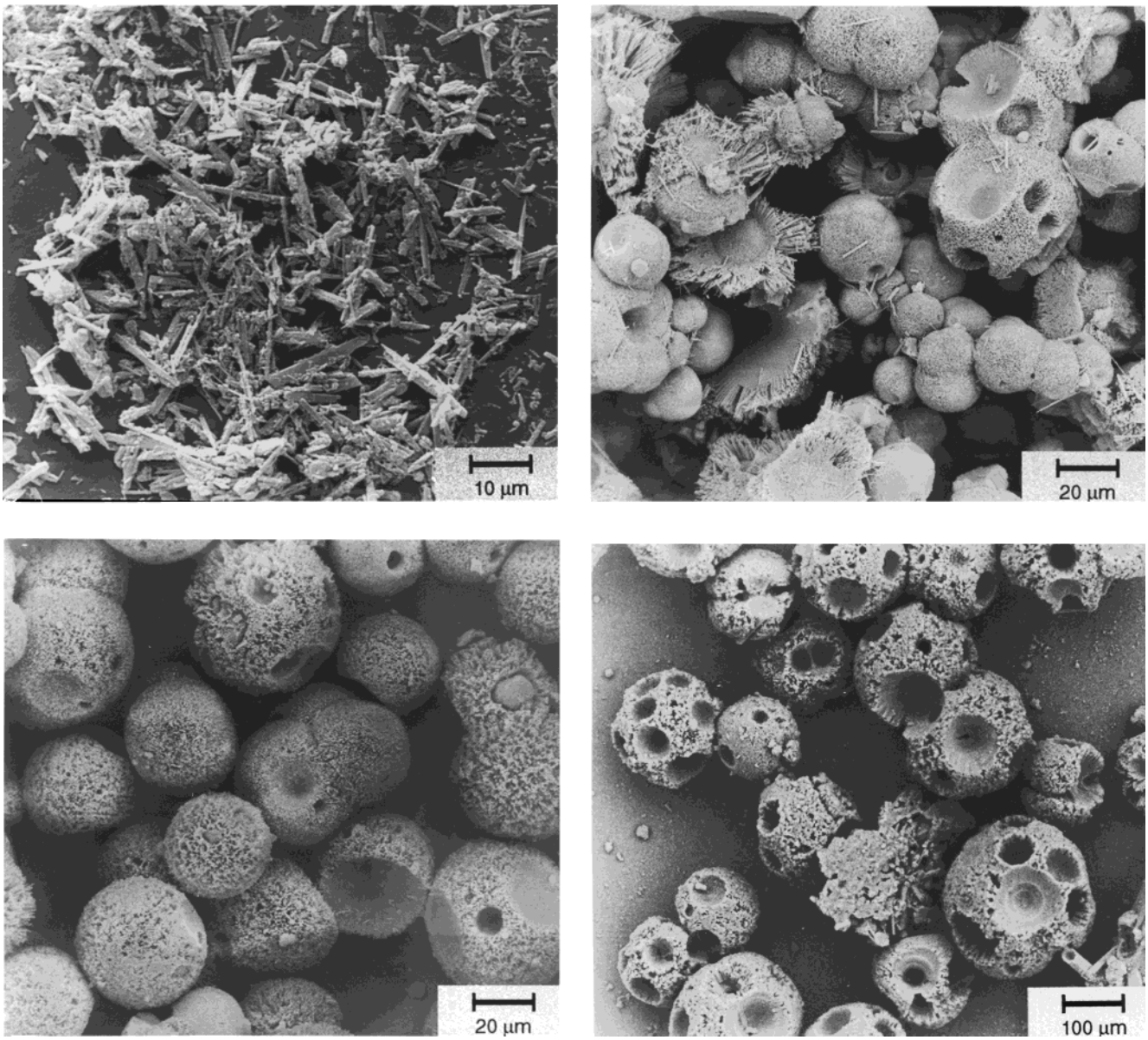

Figure 5. SEM of some samples: (a) P00, (b) P03, (c) P05, and (d) P14.

878 K. For comparison, Concepción et al.[11] found that the thermal analysis of $AlPO_4$-5 shows only two weight-loss stages corresponding to the same temperature ranges I and III of $AlPO_4$-36. The authors attributed the first stage (DTG peak I) to desorption of physisorbed water, and the same can be occurring with $AlPO_4$-36. The weight loss at region II was not observed in the well-crystallized $AlPO_4$-5,[11] and as previously stated, the crystallinity of this $AlPO_4$-36 is about 65%. So, the crystals of this sample probably have a very disordered structure and the weight loss in region II could be because of the dehydroxylation originated by defects.

The weight loss detected in $AlPO_4$-36 in stage III, as found in $AlPO_4$-5,[11] can be attributed to the decomposition of occluded amine. A weight loss at temperatures around region IV appears in the case of the AFI structure only in samples containing magnesium[11] (MAPO-5) and was attributed to the decomposition of protonated amine, which neutralizes the framework's negative charge resulting from Al^{3+} substitution by Mg^{2+}. Hence, $AlPO_4$-36 loses part of amine practically in the same region (temperature range IV) characteristic of protonated amine. This is likely because of the shape of the channels of the ATS structure, which, despite being formed by large pores, are elliptical with smaller pore diameters than those of the AFI structure and possess small lateral cavities[1] (side pockets) that restrict the amine removal.

The thermal analyses for the magnesium-containing samples (MAPO-36) are shown in Figure 6b−d (samples P26, P03, and P08) as well as in Table 6. The overall weight loss for both the $AlPO_4$-36 and MAPO-36 samples synthesized with either pseudoboehmite or aluminum isopropoxide is between 15 and 17%. The results indicate that by introducing magnesium into the ATS framework the weight loss in stage III decreases and, in parallel, the decomposition velocity in region IV becomes more intense as the magnesium content increases. This denotes a change in the species decomposed in the latter region. Considering the TG/DTG

(11) Concepción, P.; López Nieto, J. M.; Mifsud, A.; Pérez-Pariente, J. *Zeolites* **1996**, *16*, 56.

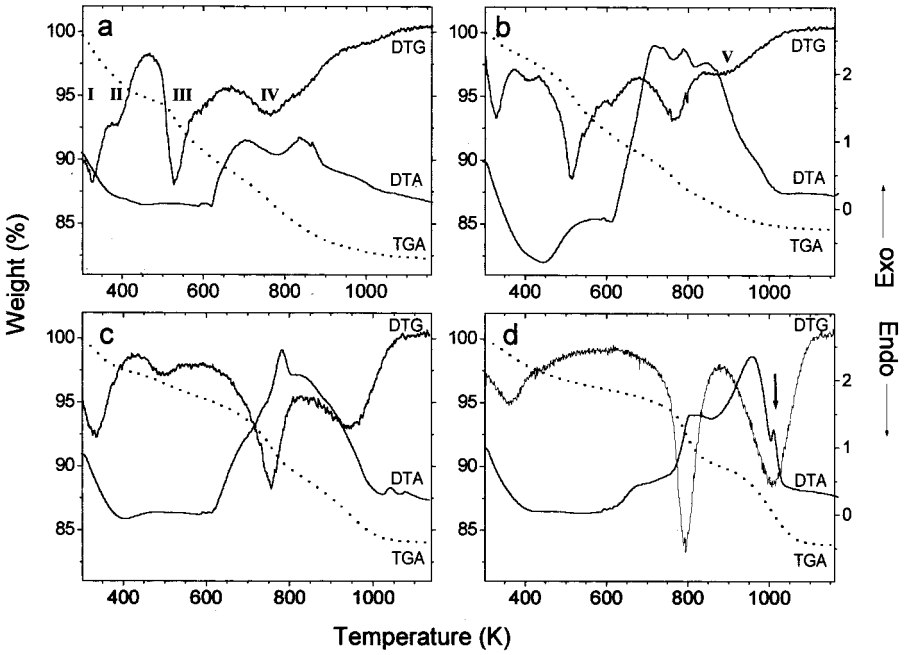

Figure 6. TGA and DTA of some selected samples: (a) P00, (b) P26, (c) P03, (d) P08.

Table 6. Percent Weight Loss from TG Analysis

sample	solid Mg/(Mg+Al+P)	temperature (K) III 473−623	IV 623−878	V 878−1173	total loss % (I to V)
P00	0.0	−4.652	−6.757	−0.030	−17.779
P26	0.012	−5.502	−5.680	−1.574	−15.415
P03	0.025	−2.371	−6.931	−3.995	−15.975
P04	0.030	−1.879	−6.691	−4.848	−16.525
P05	0.040	−1.464	−5.842	−6.009	−15.786
P06	0.042	−1.501	−5.887	−5.757	−15.654
P07	0.051	−0.857	−5.739	−6.316	−15.835
P08	0.053	−1.161	−5.918	−6.133	−16.155
P09	0.057	−0.573	−5.553	−6.539	−15.368
P11	0.074	−0.805	−5.563	−5.297	−17.093
P14	0.083		−5.493	−5.595	−15.877
I03	0.026	−1.623	−4.227	−4.632	−16.846
I04	0.035	−1.051	−4.368	−6.250	−16.20
I05	0.043	−0.908	−4.397	−6.238	−15.790
I08	0.052		−5.045	−6.845	−15.960
I09	0.061		−4.867	−7.109	−14.490

results of MAPO-5,[11] the decomposition of protonated amine in MAPO-36 may also occur in the same temperature region IV. Hence, the weight-loss behavior of region IV as the magnesium level increases (Figure 6b−d) might be attributed to a decrease of occluded amine and an increase in protonated species. Incorporation of magnesium also yields a new exothermic weight-loss stage ranging from 878 to 1173 K (peak V, Figure 6b), and as the magnesium content in the solid increases, the weight loss of stage V increases. The weight loss in stage V does not take place under inert atmosphere, indicating that it is related to the combustion of the coke formed during decomposition of the protonated amine.

For the sample with higher magnesium content in the solid (Figure 6d, sample P08), a reproducible exothermic peak appears in the DTA curve at 1053 K (indicated by an arrow), likely because of the transformation of MAPO-36 into tridimite.[12] Additional results show that the increase in magnesium content in the solid (sample P14) increases the intensity of this DTA peak, indicating

(12) Akolekar, D. B. *J. Catal.* **1994**, *146*, 62.

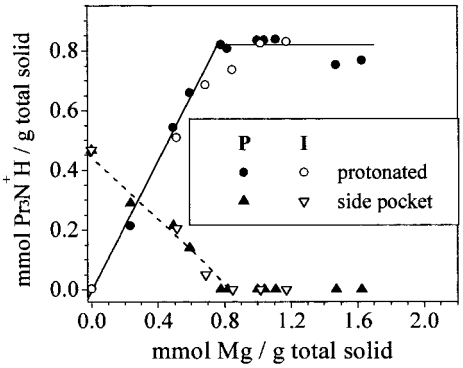

Figure 7. Amine loss in oxidant atmosphere and $T > 623$ K as a function of magnesium content in the solid (P = pseudo-boehmite and I = isopropoxide).

that the presence of magnesium facilitates the formation of this dense phase.

From the TG results presented in Table 6, it is possible to correlate the amount of protonated amine and magnesium content in the solid. As the occluded and the protonated amines desorb in the same temperature region IV, it was assumed that the weight loss corresponding to the degradation of the protonated species is proportional to coke formation (region V). The proportionality constant was determined from the samples with the highest magnesium level, which presented no occluded amine (an approximately constant ratio between the weight loss in regions IV and V). Figure 7 shows a plot corresponding to the weight loss of protonated amine, estimated in this way, as a function of the overall magnesium content in the solid. The results show that samples prepared from both aluminum sources present a linear increase of protonated amine and magnesium content up to 0.8 mmol Mg/g solid. The slope of protonated amine as a function of magnesium equals unity, indicating that for these samples Mg^{2+} cations are predominantly substituting Al^{3+} in the ATS framework. On the other hand, Figure 7 shows also that there is a linear decrease of the amine

occluded in the side pockets as the Mg content increases. Mg contents higher than 0.8 mmol Mg/g solid do not increase the weight loss corresponding to the protonated amine, indicating that from this point the magnesium atoms are located in extraframework positions. Indeed, ^{31}P NMR studies show that these samples presented nonzeolitic phosphorus signals associated to dense phosphates.[10]

Conclusions

Under the synthesis conditions employed in this work, it was observed that it is very difficult to synthesize $AlPO_4$-36 as small amounts of $AlPO_4$-5 always crystallizes parallel to this phase. Aging the reaction mixture at room temperature enhances the formation of $AlPO_4$-36 and MAPO-36. The presence of magnesium in the reaction mixture also favors the formation of the ATS structure up to a value that depends on the aluminum source (magnesium molar fraction of 0.10 in the case of pseudoboehmite and 0.05 for the aluminum isopropoxide). The synthesis of pure MAPO-36 from reaction mixtures having very low magnesium contents ($0 < y < 0.012$) was not possible under several reaction conditions. For somewhat higher magnesium contents ($0.012 < y < 0.026$), it was possible to obtain pure MAPO-36 under specific aging and crystallization periods when pseudoboehmite was the aluminum source, but this was not the case when isopropoxide was employed. Pseudoboehmite was a better aluminum source than aluminum isopropoxide for the formation of MAPO-36 as it enables one to obtain samples with much wider magnesium contents.

The thermogravimetric analysis of the ATS samples under oxidative atmosphere can show as much as five weight-loss regions. The two regions at lower temperature correspond to (I) water desorption and (II) dehydroxylation of framework defects. The three regions at higher temperatures were attributed to (III) amine desorption from side pockets, (IV) decomposition of protonated amine, and (V) coke combustion. The weight loss corresponding to decomposition of protonated amine (region IV) from samples synthesized using both aluminum sources correlates linearly very well with the magnesium content in the solid up to the value of 0.8 mmol magnesium/g solid. This suggests that up to this magnesium content the solids have an MAPO-36 molecular sieve structure, whose negative charge is compensated by the protonated amine. The solids having higher magnesium contents have approximately a constant weight loss in region IV, indicating that these additional magnesium atoms are extraframework.

Acknowledgment. We acknowledge FAPESP and CAPES for the financial support to this project.

CM9903071